

Functional consequences of mutations in the transmembrane domain and the carboxy-terminus of the murine AE1 anion exchanger

M.N. Chernova ^a, B.D. Humphreys ^{a,1}, D.H. Robinson ^a, A.K. Stuart-Tilley ^a, A.-M. Garcia ^c,
F.C. Brosius ^b, S.L. Alper ^{a,*}

^a Molecular Medicine and Renal Units, Beth Israel Hospital, Departments of Medicine and Cell Biology, Harvard Medical School, Boston, MA, USA

^b Division of Nephrology, University of Michigan Medical School, Ann Arbor, MI, USA

^c Eisai Research Institute, Andover, MA, USA

Received 23 December 1996; accepted 3 April 1997

Abstract

We have characterized mouse AE1-mediated $^{36}\text{Cl}^-$ influx and surface AE1 polypeptide expression in *Xenopus* oocytes injected with cRNA encoding two classes of loss-of-function mutants. The first arose spontaneously. Chimeric mutants constructed with a functional AE1 cDNA localized the site of spontaneous mutation to the transmembrane domain, and DNA sequencing revealed two missense mutations encoding the double-mutant polypeptide V728F/M730I. Each mutation individually produced only partial loss of AE1 transport activity, and coexpression of the individual mutants did not restore full activity. The functional changes produced by the mutations correlated with reduced fractional accumulation of polypeptides at the oocyte surface. The V728F/M730I polypeptide expressed in mammalian cells displayed complete endoH resistance and rapid degradation. We also examined the effect on AE1 function of engineered removal of its hydrophilic carboxy-terminus. Both Δ_c890 and the internal deletion $\Delta_c890-917$ were functionally inactive in *Xenopus* oocytes. Lack of transport activity correlated with lack of detectable polypeptide accumulation at the oocyte surface. Coexpression with *wt* AE1 of some, but not all, of these AE1 mutants partially suppressed *wt* AE1-mediated $^{36}\text{Cl}^-$ uptake. In contrast, coexpression with *wt* AE1 of soluble N-terminal AE1 fragments was not inhibitory. © 1997 Elsevier Science B.V.

Keywords: *Xenopus* oocyte; Chloride bicarbonate exchange; Isotopic flux; Metabolic labeling; Immunoprecipitation; Autoradiography; Mutagenesis; Plasma membrane; Chymotrypsin; Proteolysis; In vitro translation

Abbreviations: HEPES, *N*-2-hydroxyethylpiperazine-*N'*-2-ethanesulfonic acid; DIDS, 4,4'-diisothiocyanostilbene-2,2'-disulfonic acid

* Corresponding author. At: Molecular Medicine Unit RW763, Beth Israel Deaconess Medical Center, East Campus, 330 Brookline Ave., Boston, MA 02215, USA. Fax: (1) (617) 667-2913. E-mail: salper@bidmc.harvard.edu

¹ Present address: Department of Physiology and Biophysics, Case Western Reserve University School of Medicine, Cleveland, OH, USA.

1. Introduction

The band 3-related AE anion exchanger gene family includes at least three [1] and possibly four genes [2] which encode at least 14 mRNA transcripts, predicted in turn to encode at least nine polypeptide products [3–5]. Seven of these AE polypeptides are complex polytopic transmembrane proteins which mediate $\text{Cl}^-/\text{HCO}_3^-$ exchange and can serve as an-

ion exchangers of broader substrate specificity. The molecular mechanism of this anion exchange remains unknown despite the accrual over many years of much biochemical, kinetic, and molecular biological information. Our understanding of this mechanism will be greatly enhanced by knowledge of the structure of the transmembrane domains of AE proteins. Structural analysis of the red cell AE1 anion exchanger by electron microscopic tomography of reconstituted two-dimensional ordered arrays of the purified protein is proceeding through increasing levels of resolution [6]. In addition, NMR structures of individual transmembrane helices in organic solvents are being solved [7]. However, assessment of the functional consequences of mutations in AE polypeptides remains an important component of the experimental repertoire, allowing insight into the relation between protein structure and transport.

The mutations analyzed to date have been both naturally occurring and genetically engineered. Mutations in human AE1 proteins have been documented in individuals with heritable red cell shape abnormalities [8–12]. Sometimes, the mutant protein is present in the red cell membrane [8,12], but more often the mutations accompanied by hemolytic anemias are characterized by red cells lacking mutant polypeptide and with diminished total AE1 protein content [9–11]. Most of these individuals appear to be obligate heterozygotes. This reduction in AE1 content of the circulating red cell by $\geq 40\%$ predisposes to hemolysis secondary to the deficit of membrane attachment sites for the cytoskeleton [11], and perhaps also to partial destabilization of the lipid bilayer [17].

Another source of molecular variants in human AE1 has been the evaluation of red cells bearing serologically defined, low frequency blood group antigens [13–15]. Most recently, two viable AE1 null mutations have been described, one discovered in a cohort of Japanese cattle [16] and the other engineered into AE1 knockout mice [17].

Most of the AE1 mutations which result in no accumulation of mutant polypeptide are thought to result from aberrant folding during biosynthesis, or from aberrant post-translational processing. Some of the aberrant folding pathways followed by mutant polypeptides display temperature sensitivity, such that lower temperatures are permissive for expression of wild-type phenotype. Examples of the application of

this concept to recombinant expression of polytopic membrane transport proteins include surface expression of *wt* nicotinic acetylcholine receptor in fibroblasts at 28°C, but not at 37°C, [18] and surface expression in *Xenopus* oocytes of the prevalent $\Delta F508$ mutant of the cystic fibrosis transmembrane regulator protein [19]. *Xenopus* oocytes at 20°C functionally expressed both proteins which at 37°C in mammalian cells were retained in the endoplasmic reticulum. Recombinant murine AE1 has also been reported to be completely retained (though in functional form) in the endoplasmic reticulum of transiently transfected mammalian cells at 37°C [20], whereas a functionally significant fraction of AE1 accumulates at the surface of *Xenopus* oocytes [4,21–29].

In addition to reliance on functionally informative phenotypes in naturally occurring mutations, selection strategy for site-directed mutagenesis experiments designed to investigate the structural bases of AE1 transport function relies on algorithmic predictions of secondary structure deduced from primary structure and on results of chemical modification of red cells with group-specific reagents. In the course of routine plasmid subcloning in *E. coli*, we noticed a loss-of-function phenotype which arose in mouse AE1 cDNA. This paper presents the characterization of that mutation in *Xenopus* oocytes. The loss-of-function was secondary to a double mutation in residues adjacent to a residue which is mutant in human hereditary spherocytosis. These residues reside in a region of AE1 whose topography remains uncertain.

In addition, the role of the mouse AE1 carboxy-terminal cytoplasmic tail was examined in *Xenopus* oocytes. The amino-terminal cytoplasmic domain of erythroid AE1 serves as a binding site for cytoskeletal proteins, glycolytic enzymes, and denatured hemoglobin [1,2]. Removal of most of this region corresponding approximately to the membrane-proximate tryptic cleavage site produces a polypeptide which is still functional at the surface of the *Xenopus* oocyte [28]. In contrast, a physiological role for the much shorter, cytoplasmic carboxy-terminal cytoplasmic tail of AE1 [30] had not been defined. We found that removal of this carboxy-terminal tail in the form of two distinct mutations resulted in loss of transport function. In each of the two groups of mutations

studied, loss of transport function was accompanied by loss of normal surface expression of the encoded polypeptides. Thus, both groups of mutations disrupted structures required for normal cell surface accumulation of AE1 polypeptide, even in the 'permissive' *Xenopus* oocyte expression system.

Similar properties of a human AE1 mutant with a shorter deletion of the C-terminal cytoplasmic residues were reported after completion of this work [26].

2. Materials and methods

2.1. Mutagenesis and assessment of mutant polypeptides

Mouse AE1 cytoplasmic domain/transmembrane domain chimeras were constructed via the *EcoRV* site at nt 1339 (Genbank accession no. X02677). Mouse AE1 point and deletion mutants were constructed by the dut⁻, ung⁻ single-strand template method of Kunkel et al. [31] with mutagenesis kits from Amersham (Arlington Heights, IL), Stratagene (La Jolla, CA), and BioRad (Hercules, CA). The mouse AE1 point mutation G2308T was constructed using the mutagenic oligonucleotide 5'-GTTGCTG-GTCTTTGGCATGGG-3' in the AE1 fragment *Sma*I (nt 2117)–*Sph*I (nt 2678) subcloned in M13mp19. The AE1 point mutant G2316T was constructed in the same M13mp19 subclone of AE1 using the mutagenic oligonucleotide 5'-TCGTTGGCATTGGTGGG-GTGG-3'. The mutant inserts were reconstructed as cDNAs encoding full-length mutant AE1 polypeptides. The mutations were confirmed by DNA sequencing.

The AE1 C-terminal deletion mutant $\Delta 890_c$ was constructed in the AE1 fragment *Xba*I (nt 1258)–*Hind*III (nt 3911) subcloned in M13 mp19 using the mutagenic loop-out oligonucleotide 5'-GTGC-CTCTCCGTCGTTGAGCGGCAGGCCCA-3'. In this construct, AE1 residue Arg⁸⁸⁹ was followed by a terminator codon. The AE1 C-terminal internal deletion $\Delta 890-917$ was constructed in the same M13mp19 subclone of AE1 using the loop-out oligonucleotide 5'-GTGCCTCTCCGTCGTGGCCTG-GATGAATAT-3'. In this construct, AE1 residue Arg⁸⁸⁹ was followed by residue Gly⁹¹⁸. Full-length AE1 cDNAs containing each deletion mutation were

reconstructed with the *Sph*I (nt 2678)–*Hind*III (nt 3911) subfragments of each mutated insert. The integrity of the deletions was confirmed by DNA sequencing.

2.2. In vitro translation

Integrity of the mutant polypeptide products was assessed by in vitro translation in rabbit reticulocyte lysate, in the absence or presence of dog pancreatic microsomes (Promega, Madison, WI) of polypeptides labeled with [³⁵S]methionine (NEN-Dupont, Boston, MA). Translation products were analyzed by SDS-PAGE fluorography using the scintillant EnHance (NEN-DuPont). Procedures were as described previously [23].

2.3. Functional expression of heterologous AE polypeptides in *Xenopus* oocytes

cRNA was transcribed from linearized CsCl-purified plasmid DNA using kits from Stratagene and from Ambion (Austin, TX). Preparation of oocytes and microinjection with cDNAs was performed as previously described [23,27,29]. ³⁶Cl⁻ influx experiments were performed in ND-96, which contained (in mM) 96 NaCl, 2 KCl, 1.8 CaCl₂, 1 MgCl₂, and 5 N-2-hydroxyethylpiperazine-N'-2-ethanesulfonic acid (HEPES) hemisodium salt. Chemicals were from Sigma (St. Louis, MO). Uptake periods were 60 min in earlier experiments, and 15 min in later experiments. In both cases, uptakes represented initial rates. Statistical analysis of influx values for different groups of oocytes was by ANOVA, followed by *t*-tests for two samples with correction for multiple comparisons by the Fisher LSD method. ³⁶Cl⁻ efflux experiments were also performed and analyzed as previously described [24,27] as part of the determination of *K_m* for extracellular Cl⁻.

2.4. Antibodies

The affinity-purified antibody to mouse AE1 aa 214–228 was previously described [32]. The crude antiserum to mouse AE1 aa 917–929 was prepared in rabbits against peptide coupled through an added N-terminal Cys to keyhole limpet hemocyanin via the cross-linker maleimidobenzoyl-*n*-hydroxysuccinimide ester (Pierce, Rockford, IL).

2.5. Detection of AE1 and mutant AE1 at the oocyte surface

Metabolic labeling of cRNA-injected oocytes with [^{35}S]methionine (NEN) or with ^{35}S -Trans-Label (ICN, Costa Mesa, CA) was performed as previously described [23,29]. Forty-eight hours after cRNA injection, oocytes were incubated for 3 h in the absence or presence of 5 mg/ml chymotrypsin (Sigma), followed by washing, solubilization in Triton X-100, and immunoprecipitation as previously described [23]. The proportion of AE1 cleaved by exofacial proteolysis was determined by scanning densitometry using NIH Image v. 1.44. The use of surface proteolysis in this assay assumes that the mutant and truncated forms of AE1 studied retain sensitivity to exofacial chymotryptic cleavage equivalent to that of *wt* AE1. Moreover, the assay also assumes that the antibody:antigen ratios optimized for *wt* AE1 also apply to the mutant polypeptides studied below.

2.6. Construction of stable MDCK and 3T3 cell lines stably expressing AE1 V728F/M730I

The *Bam*HI fragment encoding the double-mutant AE1 polypeptide was isolated from pWB3, and subcloned into the amphotropic retroviral expression vector, pDOL. pDOL-WB3 was purified and transfected by the calcium phosphate precipitation technique into Ψ -CRIP packaging cells. Replication-deficient recombinant retrovirus released into the tissue culture supernatant was used to infect MDCKII cells and 3T3 cells. Infected cells were selected in humidified 5% CO_2 in MEM (Gibco, Bethesda, MD) containing 10% calf serum and G418 (Gibco) at 0.6 mg/ml for MDCK cells and at 0.2 mg/ml for 3T3 cells. Individual G418-resistant colonies were isolated with plastic cloning rings, cloned, amplified in the continued presence of G418, and screened for mouse AE1 expression by northern blot and by immunoblot.

2.7. Pulse-chase experiments for determination of AE1 half-life and *endoH* resistance

MDCK cell clones and 3T3 cell clones overexpressing human AE1 V728F/M730I were incubated

for 30 min in methionine-free DME medium (Gibco), followed by 20 min in the same medium supplemented with 250 $\mu\text{Ci/ml}$ [^{35}S]methionine (pulse period). Cells were then rinsed with methionine-free DME, and normal MEM was restored for the indicated chase times. Labeled cells were solubilized in 1% NP-40 lysis buffer containing (in mM) 140 NaCl, 20 sodium phosphate, 2 PMSF, and 1 EGTA. Lysates were cleared by centrifugation in a microfuge for 30 min at 18 000 rpm at 4°C. Cleared lysates were precleared with protein A-Sepharose (Sigma), then incubated for 2 h at 4°C with affinity-purified anti-mouse AE1 aa 917–929. After an additional 30-min incubation with protein A-Sepharose, the antibody–antigen–bead complexes were isolated, suspended in SDS–PAGE load buffer, and subjected to SDS–PAGE on 10% acrylamide gels [22,23].

3. Results

3.1. Assignment of a spontaneous loss-of-function in AE1 to mutations in its transmembrane domain

The cDNA encoding mouse erythroid AE1 [33] was subcloned from its original pUC13 carrier into the transcription vector pSP64 to generate the recombinant plasmid, pWB3. cRNA transcribed from linearized templates of this plasmid were injected into *Xenopus* oocytes for assessment of functional expression. However, pWB3 cRNA did not confer on oocytes the incremental transport of ^{36}Cl -expected for mouse erythroid AE1 (eAE1) [21]. In subsequent experiments [22], cDNA cloning of mouse kidney AE1 (kAE1) revealed a translational initiation site at Met⁸⁰ of the eAE1 amino acid sequence. cRNA transcribed from the kAE1 plasmid subclone pL2A was expressed in *Xenopus* oocytes and conferred on these oocytes increased ^{36}Cl -uptake which was blocked by addition of the transport antagonist, 4,4'-diisothiocyano-stilbene-2,2'-disulfonic acid (DIDS).

In order to test the hypothesis that the functional difference between erythroid AE1 cRNA transcribed from pWB3 and kidney AE1 cRNA transcribed from pL2A originated in a mutation in the pWB3 cDNA, chimeric cDNAs were constructed, the corresponding cRNAs were expressed in *Xenopus* oocytes, and the

oocytes were subjected to assays of $^{36}\text{Cl}^-$ influx. Fig. 1A shows the parental and chimeric constructs tested. pBL contained the N-terminal cytoplasmic domain from pWB3 and the C-terminal transmembrane domain from pL2A. The converse construct, pLB, contained the N-terminal cytoplasmic domain from pL2A and the C-terminal transmembrane domain from pWB3. Fig. 1B shows that oocytes injected 48 h earlier with cRNAs from plasmids pWB3 and pLB did not differ in $^{36}\text{Cl}^-$ uptake from oocytes injected with water ($P > 0.5$). In contrast, oocytes expressing erythroid AE1 from the chimeric construct pBL ($P < 0.00001$) and oocytes expressing kidney AE1 from plasmid pL2A ($P = 0.02$) both displayed $^{36}\text{Cl}^-$ uptake exceeding that of water-injected oocytes².

This result suggested the presence of one or more mutations in the AE1 transmembrane domain in plasmid pWB3. This hypothesis was confirmed by DNA sequencing of pWB3 and pL2A between nt 1213 (*EcoRV*) and nt 3006 (*BglII*) of the murine AE1 sequence, encoding the region from aa 404 to beyond the C-terminal aa 929 into the 3'-untranslated region. This comparison revealed two missense mutations in pWB3, G2308T and G2316T. The cDNA containing these mutations encoded the double mutant AE1 polypeptide V728F/M730I. Residues 728 and 730 of mouse AE1 are situated in putative transmembrane span 9 (TM9) in the postulated 14 transmembrane span model of AE1, a still-debated model based on hydropathy analysis, antibody reactivities, chemical modification, and proteolytic susceptibilities [26,34]. However, the region between putative TM8 and TM11 is topographically the least well defined of the AE1 polypeptide. This region of the protein may span the lipid bilayer one or three times, with transmembrane spans of uncertain length.

² In Fig. 1B, the $^{36}\text{Cl}^-$ uptake activity displayed by oocytes previously injected with cRNA transcribed from pL2A, though significantly elevated compared to water-injected oocytes and pWB3-expressing oocytes, is less than observed in oocytes of the same experiment previously injected with cRNA transcribed from pBL. This difference in expression level between pL2A-programmed oocytes and oocytes programmed with pBL [27] or with anemic spleen mRNA [22] was not borne out in later experiments.

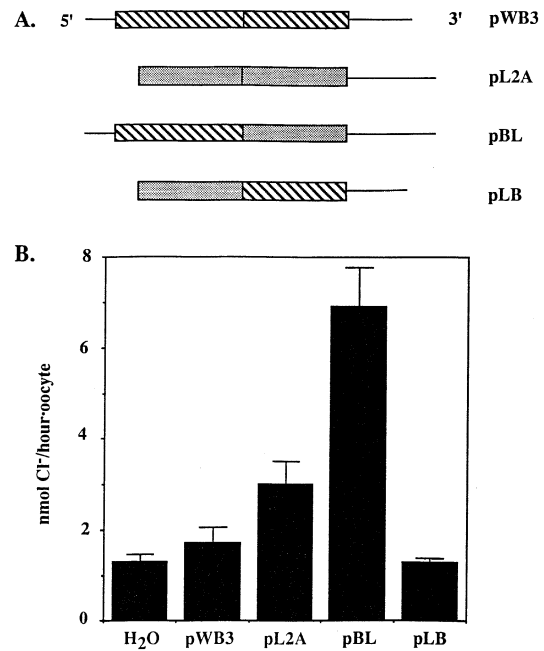


Fig. 1. A: schematic of cRNAs expressed in *Xenopus* oocytes to define region of AE1 in which spontaneous mutation led to loss of function. pWB3 (cross-hatched), mutant mouse erythroid AE1 plasmid; pL2A, mouse kidney AE1 plasmid (shaded). pBL and pLB are chimeras of complementary structure as indicated. B: $^{36}\text{Cl}^-$ influx into oocytes injected with the cRNA products of the indicated plasmids or with water. The chimera pBL expressed Cl^- uptake, whereas the chimera pLB was inactive. Values are means \pm S.E.M.

3.2. Determination of the roles of the individually mutated amino acid residues 728 and 730

The individual AE1 mutations V728F and M730I were constructed in a wt AE1 (pBL) background. Fig. 2 shows in vitro translations which confirmed that cRNA transcribed from each mutant plasmid encoded a full-length AE1 polypeptide. As shown in lanes 5, 7, and 9, AE1 V728F, AE1 M730I, and the AE1 double mutant each encoded a polypeptide with a mobility on SDS-PAGE close to or equal to that of wt AE1 (lane 1), with a leading edge at ~ 105 kDa. The double mutant V728F/M730I (lane 9) accumulated to the same degree as did wt AE1 (lane 1), though the single mutants accumulated to lower degrees. As previously observed with human AE1, in vitro translation in the absence of microsomes [23,35] produced decreased yields of AE1 polypeptide (even-numbered lanes).

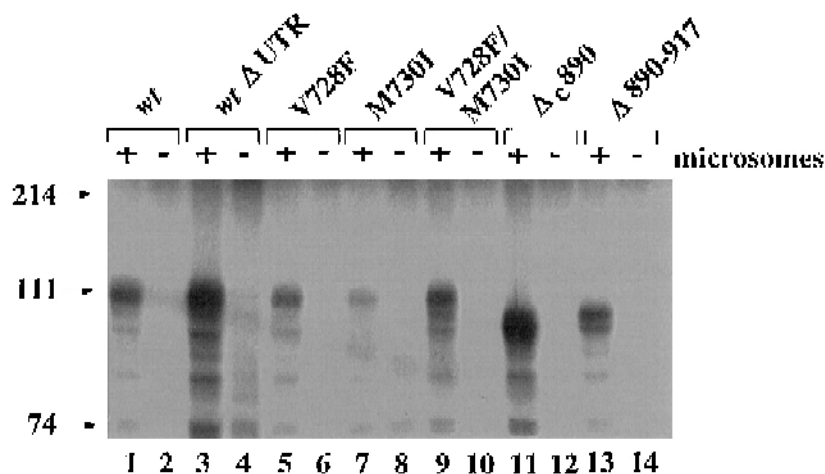


Fig. 2. In vitro translation of AE1 polypeptides from cRNA templates encoding the indicated AE1 constructs, in the presence and absence of pancreatic microsomes. Full-length translation products are the major bands in each lane containing microsomes (~ 105 kDa, or slightly lower in lanes 11 and 13). Smaller bands likely represent products of premature chain termination and/or proteolytic degradation. Molecular mass markers are indicated at the left.

3.3. Biosynthetic accumulation and surface expression of mouse AE1 in *Xenopus* oocytes

Biochemical evidence for the heterologous expression of human erythroid AE1 at the surface of *Xenopus* oocytes has been demonstrated by exofacial cleavage with chymotrypsin [23,25,26]. However, although functional expression of mouse AE1 in *Xenopus* oocytes has been documented [21,22,27], biochemical evidence for oocyte surface expression of the mouse AE1 polypeptide has not been presented [4]. For this reason, and in order to evaluate the causes of the loss-of-function phenotype of mutant AE1 encoded by pWB3, oocytes expressing mouse erythroid AE1 were metabolically labeled, exposed to chymotrypsin, and detergent-solubilized. Cleared oocyte lysates were then subjected to immunoprecipitation with antipeptide antibodies to mouse AE1 residues 214–228 in the N-terminal cytoplasmic domain [32], and to mouse AE1 cytoplasmic C-terminal residues 917–929 (see Section 2: Materials and methods).

Fig. 3 demonstrates that mouse AE1 is immunoprecipitated by both antibodies to residues 917–929 (lane 1) and to residues 214–228 (lane 2). However, after exofacial chymotryptic digestion, antibody to residues 214–228 also precipitates the non-glycosylated N-terminal 60-kDa fragment generated by

cleavage in the exofacial loop between putative TM5 and TM6 (lane 5). In contrast, antibody to C-terminal residues 917–929 fails to precipitate the 60-kDa fragment, but recognizes the more diffuse, C-terminal 35-kDa chymotryptic fragment which is heterogeneously glycosylated (lane 4). Second rounds of immunoprecipitation with excess antibody failed to precipitate additional holo-AE1 or proteolytic fragments. The fainter, more diffuse quality of the 35-kDa C-terminal chymotryptic fragment autoradiographic band led to the decision to follow the N-terminal 60-kDa chymotryptic fragment as the biochemical index of AE1 expression at the oocyte surface in subsequent experiments.

3.4. Functional expression of AE1 mutants V728F and M730I and the double mutant

Fig. 4 shows that each single mutation, V728F and M730I, allowed continued expression of AE1-mediated $^{36}\text{Cl}^-$ uptake, but at only a fraction of the level of wild-type AE1 function. In a total of 4 similar experiments each involving 8–12 oocytes per group, V728F and M730I expressed 28 ± 14 and $41 \pm 12\%$, respectively, of *wt* AE1 function measured as $^{36}\text{Cl}^-$ uptake. The individual mutations resulted in minimal (statistically insignificant) changes in K_m for extracellular Cl^- , 4.4 ± 1.2 mM (S.E.M., $n = 3$) for *wt*

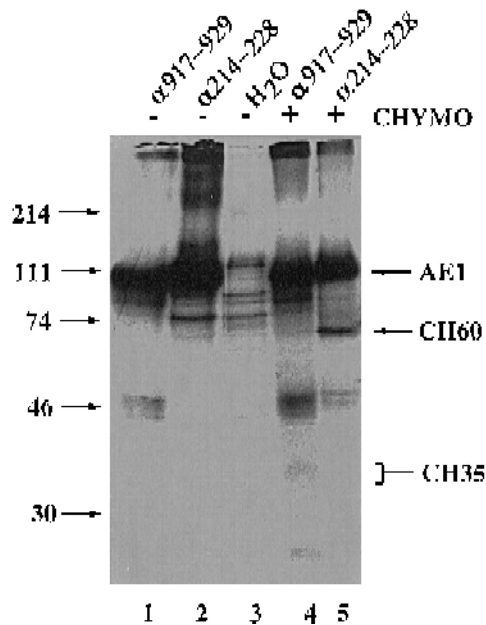


Fig. 3. Expression of mouse AE1 at the surface of *Xenopus* oocytes. Intact oocytes expressing wt AE1 and metabolically labeled with [35 S]methionine were incubated in the absence or presence of chymotrypsin, then solubilized and subjected to immunoprecipitation with the indicated anti-AE1 antipeptide antibodies. AE1 holoprotein and the N-terminal CH60 fragment are indicated by arrows (right). The glycosylated C-terminal CH35 fragment is indicated by a bracket (right). Molecular mass markers are indicated at the left.

AE1 vs. 8.8 ± 2.9 mM ($n = 2$) for V728F ($P = 0.19$ vs. wt) and 8.4 ± 1.2 mM ($n = 4$) for M730I ($P = 0.07$ vs. wt).

Coinjection into *Xenopus* oocytes of V728F with M730I at a molar ratio of 1:1 exhibited neither functional complementation nor inhibition, with $^{36}\text{Cl}^-$ uptakes comparable to those of either mutant alone. Coinjection with wt AE1 cRNA of V728F at 1:1 cRNA ratio resulted in partial inhibition of wt AE1 transport activity ($P = 0.0002$), with greater inhibition when the V728F/wt AE1 cRNA ratio was 5:1 ($P = 0.01$ compared to 1:1 coinjection). The double mutant V728F/M730I was itself inactive in *Xenopus* oocytes. When coexpressed with wt AE1 cRNA at 1:1 cRNA ratio, the double mutant produced minimal inhibition of AE1-mediated $^{36}\text{Cl}^-$ uptake ($P > 0.2$). However, at a cRNA molar ratio of 5:1 the double mutant inhibited wt AE1 function in these assay conditions by $\sim 35\%$ ($P = 0.00001$). Interestingly, the degree of inhibition produced by coexpress-

sion with wt AE1 of V728F/M730I was less than that produced by coexpression of V728F at ratios of 1:1 ($P = 0.017$) or 1:5 ($P = 0.037$). This may relate to the lesser accumulation of doubly mutant polypeptide that could serve to decrease stability and/or efficiency of trafficking of wt AE1 polypeptide in the oocyte.

To determine the degree to which reduced surface expression of AE1 polypeptides could explain the decreased functional activities of the above AE1 mutant polypeptides, the levels of accumulation of the AE1 polypeptides in the oocytes, and their susceptibility to exofacial digestion with chymotrypsin were examined. As shown in Fig. 5, both V728F (lane 3) and M730I (lane 5) accumulated to lower levels than did wt AE1 (lane 1), whereas accumulation of the double mutant polypeptide V728F/M730I was yet more severely reduced (lane 7). The proportion of total oocyte AE1 cleaved by exofacial digestion of oocytes to yield the N-terminal chymotryptic fragment P60 was reduced to 7% in oocytes expressing

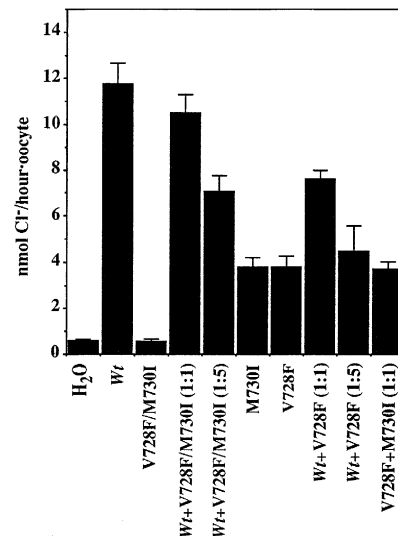


Fig. 4. $^{36}\text{Cl}^-$ influx into *Xenopus* oocytes mediated by wt AE1 ($n = 23$), the spontaneous AE1 double mutant V728F/M730I ($n = 22$) and AE1 polypeptides with each of the individual mutations singly and coexpressed ($n = 11$ or 12). Also shown are effects on wt AE1 function of coexpression of V728F/M730I and of V728F at mutant:wt molar ratios of 1:1 and 5:1 ($n = 11$ –13). The double mutation produced loss of function and the single mutations reduced function. However, V728F appeared a stronger inhibitor of wt AE1 function than V728F/M730I. Values are means \pm S.E.M.

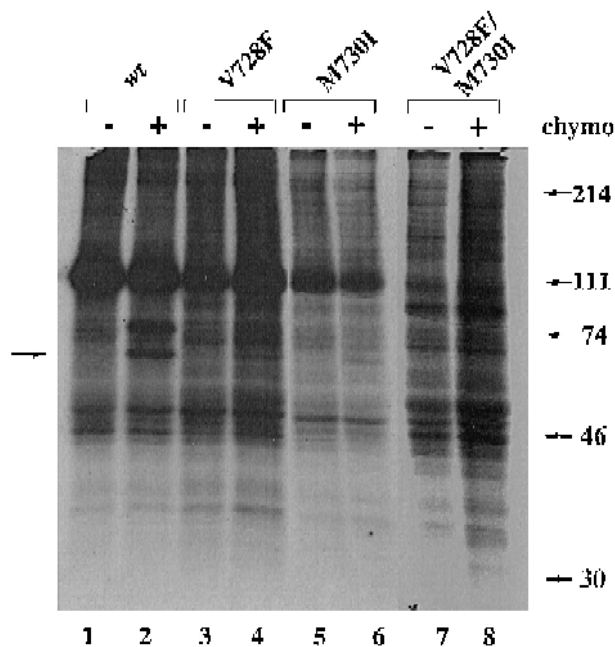


Fig. 5. Surface expression in *Xenopus* oocytes of the AE1 mutant polypeptides V728F, M730I, and the double mutant. Procedures were as in Fig. 3. Arrow at the left indicates the N-terminal AE1 chymotryptic fragment, CH60. Molecular mass markers are indicated at the right.

either single mutant V728F or M730I (lanes 4 and 6, respectively) compared to 15% for *wt* AE1. P60 generated from the double mutant V728F/M730I was below the threshold of detection (lane 8) even upon prolonged exposure (not shown).

These results suggested that the decreased $^{36}\text{Cl}^-$ transport measured in oocytes expressing AE1 V728F or M730I could be largely attributed to decreased quantity of mutant polypeptide at the oocyte surface compared to *wt* AE1 polypeptide. The near absence of $^{36}\text{Cl}^-$ transport measured in oocytes expressing the double mutant polypeptide V728F/M730I could be attributed to severely decreased accumulation of mutant polypeptide. The decreased accumulation of mutant polypeptides could have been secondary to decreased rates of biosynthesis or trafficking to the surface, or to decreased stability at the surface or prior to arrival at the surface. The near-normal accumulation of the double mutant polypeptide in dog pancreas microsomes *in vitro* (Fig. 2) suggests that the locus of altered trafficking or altered susceptibility to degradation is postendoplasmic reticulum.

3.5. AE1 V728F/M730I exhibits rapid turnover in mammalian cells

The discovery of the double point mutation in pWB3 led to a new understanding of the kinetic behavior of mouse AE1 stably transfected into MDCK cells. Multiple clonal lines expressing AE1 were produced using an expression vector in which the AE1-coding portion was derived from pWB3. Thus, the transfected AE1 turned out to contain the double point mutation. As shown in Fig. 6A, the AE1 polypeptide in these cells exhibited a half-life of ≤ 2 h. Fig. 6B presents a possible explanation for this short half-life. The heterologous AE1 V728F/M730I was retained in the endoplasmic reticulum or the *cis*-Golgi, since it remained completely susceptible to digestion by endoglycosidase H even after 75 min of chase. Consistent with this apparent sequestration inside the cell, AE1 V728F/M730I in MDCK cells was not susceptible to proteolysis by extracellular chymotrypsin (not shown). Comparable results were obtained in multiple independent clones of mouse 3T3 cell stably transfected with mouse AE1 (not shown) and in transiently transfected HEK-293 cells [20]. If AE1 V728F/M730I expressed in *Xenopus* oocytes were similarly unable to leave the endoplasmic reticulum, becoming subject to accelerated prote-

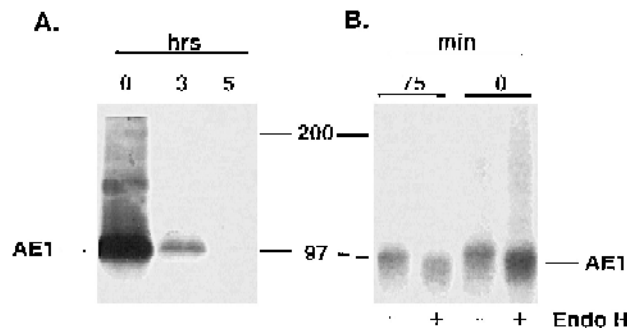


Fig. 6. Instability of the protein product of pcDNA1-WB3 stably transfected into MDCK cells. A: immunoprecipitation of heterologous mouse AE1 from whole cell lysates of stably transfected MDCK cells after labeling with [^{35}S]methionine for 2 h, followed by chase times of 0, 3, or 5 h. Similar results were observed in three independent, clonal cell lines. B: endoglycosidase H susceptibility of ^{35}S -labeled heterologous mouse AE1 from MDCK cell lysates after chase times of 0 or 75 min. Similar results were obtained in experiments with five independent, clonal cell lines.

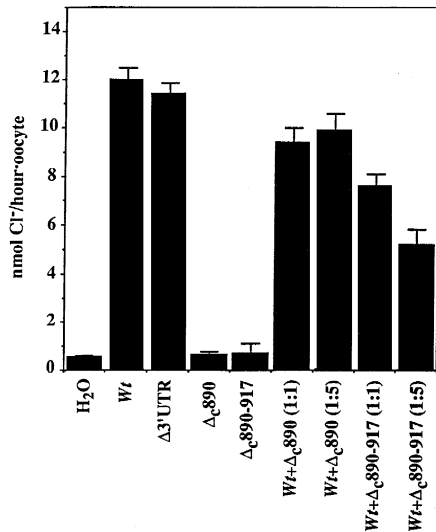


Fig. 7. $^{36}\text{Cl}^-$ influx into *Xenopus* oocytes mediated by the AE1 carboxy-terminal truncation mutants Δ_{c890} ($n = 23$) and $\Delta_{890-917}$ ($n = 22$) compared with wt AE1 ($n = 9$) and with $\Delta 3'$ -UTR ($n = 21$). Also shown are effects of mutant coexpression on wt AE1 function at mutant:wt molar ratios of 1:1 and 5:1 ($n = 9-10$). All mutant constructs shown in this figure lack the mouse AE1 3'-UTR. Both truncations produced loss of function, but only $\Delta_{890-917}$ substantially inhibited coexpressed wt AE1. Values are means \pm S.E.M.

olytic degradation, its lack of accumulation would be explained.

3.6. Functional consequences of removal of the carboxy-terminal cytoplasmic tail of AE1

Though AE1 has two cytoplasmic domains, most attention has focused on the larger N-terminal cytoplasmic domain, known to mediate important cytoskeletal binding functions. The function if any, of the short C-terminal cytoplasmic domain had not been addressed experimentally. In order to examine the functional necessity of the presence of the C-terminal cytoplasmic domain, C-terminal truncations of mouse AE1 were constructed which also lacked the portion of the 3'-untranslated region (nt 2791–3785) present in the constructs presented above. Fig. 7 shows that though deletion of only this portion of the 3'-untranslated region from the AE1 cRNA ($\Delta 3'$ -UTR) produced no diminution in AE1-mediated $^{36}\text{Cl}^-$ uptake, removal of the C-terminal 39 amino acids following R889 completely abolished transport function (Δ_{c890}). Attachment of the C-terminal residues 918–

929 directly to R889 produced no further increase in $^{36}\text{Cl}^-$ uptake ($\Delta_{890-917}$).

Fig. 7 also shows the results of coexpression of these mutant AE1 polypeptides with wt AE1. Δ_{c890} coexpression slightly inhibited wt AE1 function whether at 1:1 ($P > 0.0004$) or 5:1 molar cRNA ratios ($P > 0.04$), but these degrees of inhibition did not differ ($P = 0.47$). Coexpression of $\Delta_{890-917}$ with wt AE1 at a 1:1 molar cRNA ratio showed greater inhibition of wt AE1 function ($P < 0.0005$), and the degree of inhibition increased when mutant cRNA exceeded wt cRNA by a 5:1 molar ratio ($P < 10^{-6}$ compared to 1:1).

Metabolic labeling and immunoprecipitation were again used to evaluate the degree to which the loss-of-function which accompanied deletion of C-terminal residues of AE1 could be explained by defects in polypeptide biosynthesis or in oocyte surface expression. Fig. 2 demonstrates that in the presence of microsomes, Δ_{c890} accumulated to wt levels, but that $\Delta_{890-917}$ showed reduced accumulation (lanes 11–14). Fig. 8 compares oocyte surface expression of

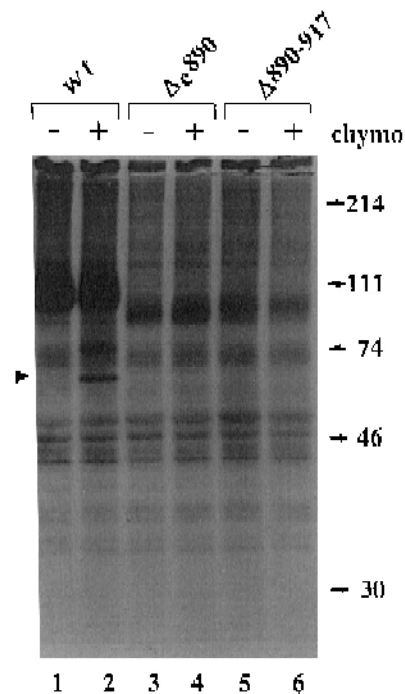


Fig. 8. Surface expression in *Xenopus* oocytes of the AE1 mutant polypeptides Δ_{c890} and $\Delta_{890-917}$. Arrowhead (left) indicates the N-terminal AE1 chymotryptic fragment, CH60. Molecular mass markers are indicated at the right.

wt AE1 with that of Δ_c890 and of $\Delta890$ –917. Total accumulation of both truncated AE1 polypeptides was substantially reduced compared to *wt* AE1. Generation of CH60 by exofacial chymotryptic cleavage of the truncated AE1 polypeptides was below the threshold of autoradiographic detection. Thus, decreased accumulation and decreased surface delivery of mutant AE1 polypeptides Δ_c890 and of $\Delta890$ –917 likely suffices to explain the absence of increased $^{36}\text{Cl}^-$ uptake by oocytes which express them.

Inhibition of *wt* AE1 function by $\Delta890$ –917 was not replicated by coexpression of N-terminal soluble fragments of AE1. Coexpression of neither the entire N-terminal cytoplasmic domain of AE1 (Δ_c405 , amino acid residues 1–405, $n = 3$ frogs, 25 oocytes) nor of the shorter N-terminal fragment Δ_c122 ($n = 1$ frog, 10 oocytes) produced any inhibition of *wt* mouse AE1 function. The polypeptides encoded by both of these truncated AE1 cRNAs stably accumulated in reticulocyte lysate translation reactions (not shown). Curiously, however, when coexpressed with *wt* human AE1, mouse AE1 Δ_c405 did produce mild inhibition of *wt* transport function [23].

4. Discussion

This paper presents a functional analysis of mutations in two regions of the mouse AE1 anion exchanger polypeptide. The first region is in putative transmembrane span 9, and was detected in the course of examining a spontaneously arising AE1 cDNA which exhibited a loss-of-function phenotype. The second region is the carboxy-terminal cytoplasmic tail of AE1. Mutations in both regions either reduced or abolished AE1-mediated $^{36}\text{Cl}^-$ influx in *Xenopus* oocytes. Reduction or loss of function paralleled and could be explained by reduction or loss of accumulation of AE1 polypeptide in the oocyte plasma membrane. The double mutant in putative transmembrane span 9 was also impaired in trafficking and short-lived in transfected MDCK cells and 3T3 cells.

4.1. Mutations in AE1 residues 728 and 730

The loss-of-function double mutant, V728F/M730I, arose in a region of AE1 with still unknown topography and function. That region is

often described for convenience as transmembrane span 9. The topographical dispositions of the putative seventh and eighth transmembrane spans of AE1 are determined by the presence in the exofacial loop connecting them of N-linked glycan and of serological blood group determinants [13,15]. Their predicted topographical disposition is further supported by the ability of transmembrane span 7 to express signal sequence function [35]. The integrity of the cytoplasmic loop between putative transmembrane spans 8 and 9 has been shown necessary for delivery of functional AE1 to the *Xenopus* oocyte surface in the absence of coexpressed glycophorin A [26]. However, human AE1 residue E681 (mouse E699) is also accessible to the extracellular aqueous space, and constitutes part of the anion translocation pathway [24,36,37]. More distally from the site of the double mutation, the region around human AE1 K743 (mouse K761) has been defined as cytoplasmic by intracellular trypsinization [38]. This site is not susceptible to exofacial trypsinization in mouse AE1 and AE2 expressed in *Xenopus* oocytes (Chernova and Alper, unpublished). The same tryptic site has also been found in the corresponding region of porcine AE2 [39]. It remains uncertain whether the putative transmembrane spans 9–12 portrayed in the model of Wood [34] and by others in fact comprise 4 or only 2 transmembrane spans.

Interestingly, there exists a human AE1 mutant allele associated with hereditary spherocytic anemia, Band 3 Prague VIII, which encodes L707P [9], corresponding to residue 725 in the mouse. Mouse L725 is predicted to interact with V728 (the site of one of the mutations in pWB3) on the same surface of putative transmembrane helix 9 of AE1. The red cells in this autosomal dominant, obligately heterozygous syndrome, contain decreased levels of AE1 polypeptide (the mutant polypeptide was likely absent), though the mutant mRNA was detected in blood by reverse transcriptase-PCR. Thus, like mouse AE1 V728F/M730I expressed in *Xenopus* oocytes and in mammalian cells, human AE1 L707P in erythroid precursor cells may exhibit instability secondary to altered protein folding or helix packing.

Each single mutation in isolation, V728F and M730I, produced a $\sim 60\%$ decrease in transport function in *Xenopus* oocytes. When coexpressed, neither of the single mutants complemented the other.

Though the double missense mutation could have arisen by chance, there are several indications that the host *Escherichia coli* strain harboring the recombinant mutant plasmid might have had a growth advantage over bacteria harboring either the recombinant *wt* AE1 plasmid or the single point mutants. In particular, constitutive overexpression in *E. coli* of human erythroid AE1 N-terminal cytoplasmic domain has proved toxic to *E. coli* [40], whereas overexpression of human kidney AE1 cytoplasmic domain, lacking the 65 N-terminal amino acid residues of the erythroid isoform, was compatible with bacterial survival [41]. Similarly, high-level expression in *Saccharomyces cerevisiae* of the full-length mouse erythroid AE1 polypeptide was unsuccessful, though removal of the N-terminal 183 amino acid residues allowed overexpression of functional anion exchanger polypeptide to high levels [42].

AE1 cytoplasmic domain-mediated toxicity in *E. coli* might result from inhibition of glycolysis via sequestration of aldolase [42] or glyceraldehyde dehydrogenase (GAPDH [43]). Mammalian GAPDH has also been reported to exhibit microtubule bundling/unbundling activity, sarcolemmal t-tubule protein kinase activity, single-stranded DNA binding activity [43], and weak uracil DNA-glycosylase (UDG) activity [44], important to DNA repair.

The impaired accumulation of the AE1 V728F/M730I doubly mutant polypeptide and its absence at the surface of the *Xenopus* oocytes and mammalian cells might clarify the long-standing suggestion that the plasma membrane protein sorting machinery of non-erythroid mammalian cells, as opposed to that of *Xenopus* oocytes, could not deliver *wt* AE1 to the plasma membrane [20,39]. Interestingly, the same group of investigators reported without further comment the successful plasmalemmal expression of *wt* murine AE1 as part of a more recent study [45]. This discrepancy might well be explained by their inadvertent use of AE1 V728F/M730I or another loss-of-function mutant for the earlier studies, whereas a *wt* cDNA might have been used for the latter study.

A similar discrepancy has been presented for AE1 expression in *S. cerevisiae* [42,46]. Thus, overexpression of a variant of murine AE1 led to accumulation in internal compartments, without delivery of the heterologous polypeptide to the plasma membrane

[42]. In contrast, a later report of overexpression of the human AE1 transmembrane domain (albeit at lower expression level) successfully achieved functional expression of the heterologous polypeptide at the yeast plasma membrane [46]. Perhaps mouse AE1 V728F/M730I or another loss-of-function mutant was used in the earlier *S. cerevisiae* study.

4.2. Mutations at the AE1 carboxy-terminus

The second class of mouse AE1 mutants examined in the present study was a pair of truncations of the carboxy-terminal cytoplasmic region. These truncated mouse AE1 polypeptides were accumulated in reticulocyte lysates and integrated into microsomal membranes. In oocytes, however, total polypeptide accumulation was reduced, and no mutant polypeptide was detectable at the oocyte surface by proteolytic cleavage. The lack of accumulation at the oocyte surface of mouse AE1 lacking residues 890–917 and 890–929 is consistent with the finding [26] that human AE1 lacking residues 882–911 presented a similar phenotype in *Xenopus* oocytes: absence of $^{36}\text{Cl}^-$ influx, somewhat diminished accumulation of polypeptide, and absence of detectable surface expression of polypeptide, not subject to rescue by coexpressed glycophorin A.

Interestingly, the human AE1 hereditary spherocytosis-associated mutation, R870W, is adjacent to R871. This latter arginine residue corresponds to mouse R889 and terminates the human equivalent of the mouse AE1 mutant $\Delta_{\text{C}}890$. Human AE1 R870W seems to be an obligate heterozygous mutation in which mutant mRNA is present in reticulocytes, but mutant protein appears to be absent in mature red cells [23].

The apparently lower total accumulation of the murine AE1 mutant polypeptides $\Delta_{\text{C}}890$ and $\Delta_{\text{C}}890$ –917 in *Xenopus* oocytes compared with human AE1 $\Delta_{\text{C}}881$ [26] may relate to the topography of the C-terminal transmembrane span. Murine $\Delta_{\text{C}}890$ terminates with Arg–Arg, suggesting a tryptic site in *wt* AE1 which might be located at the cytoplasmic surface of the lipid bilayer. Human $\Delta_{\text{C}}881$ corresponds to murine $\Delta_{\text{C}}898$, and terminates in both species with the dipeptide Arg–Glu.

The addition of residues 918–929 to residue 889 of mouse AE1 in the mutant $\Delta_{\text{C}}890$ did not rescue

the loss-of-function phenotype in the present study. Rather, the presence of residues 918–929 appeared to increase the mutant's inhibitory effect when coexpressed with *wt* AE1 (Fig. 7). Taken together with the proteolytic susceptibility of the AE1 C-terminus (see below), these data are compatible with the C-terminal amino acids serving as a site of intramolecular or intermolecular interaction with another domain of AE1 or with another polypeptide.

Mori et al. [47] reported on the proteolytic susceptibility of this carboxy-terminal region of AE1, building on their earlier characterization of tryptic peptides of the AE1 transmembrane domain which became protease-susceptible only following membrane treatment with NaOH. Pretreatment of membranes with 10 mM NaOH, a concentration which preserved the ability of AE1 to bind to the extracellular antagonist H₂DIDS and undergo intramolecular crosslinking, allowed subsequent proteolytic release of 27% of the human AE1 carboxy-terminal peptide Ala⁸⁹³–Val⁹¹¹ (corresponding to mouse AE1 Val⁹¹¹–Val⁹²⁹). Pretreatment of membranes with 40–100 mM NaOH allowed subsequent proteolytic release of up to 85% of this carboxy-terminal peptide. Similar patterns were observed for proteolytic release of five additional peptides encoding putative hydrophilic loops connecting transmembrane segments [48]. In contrast, only 25% of the human AE1 tryptic peptide Asn⁸⁸⁰–Lys⁸⁹² (corresponding to mouse AE1 E898–K910) was released upon digestion of membranes previously treated with 100 mM NaOH. Moreover, the candidate tryptic site Arg⁹⁰¹–Asp⁹⁰² (which in the corresponding sequence Leu⁹¹⁹–Asp⁹²⁰ of mouse AE1 is not a tryptic site) was resistant to digestion even following membrane pretreatment with 100 mM NaOH [47].

The degree of alkali resistance of tryptic sites can be considered an inverse index of the degree of exposure of that site within the polypeptide in the context of the membrane. In this light, the inability to detect in alkali-treated membranes any peptide generated from tryptic cleavage at human AE1 Arg⁸⁷⁰–Arg⁸⁷¹ also suggests that this site is shielded. Since seven hydrophobic residues follow human AE1 Arg⁸⁷¹ (and mouse R889), the cytoplasmic terminus putative TM14 is likely nearer to human AE1 Arg⁸⁷⁹ (mouse R897) than to human Arg⁸⁷¹ (mouse R889). Mori et al. [47] suggested that the sequence (V/L)EXXXLD(A/G)DD, found in the carboxy-

terminal cytoplasmic regions both of AQP1 and of human and mouse AE1, might contribute to a role of the C-terminal cytoplasmic region in trafficking to the cell surface. Removal of the carboxy-terminal cytoplasmic tail of AQP1 (containing the above sequence) also led to AQP1 retention within the *Xenopus* oocyte.

It was of interest to assess the effects on *wt* AE1 function of coexpression of mutant AE1 polypeptides, since AE1 solubilized in non-ionic detergent from the red cell membrane exists as dimers and tetramers [6,26,40,49], and the AE1 mutant Southeast Asian Ovalocytosis (Δ 400–408) forms hetero-oligomers with *wt* AE1 [49]. The loss-of-function mutants studied did inhibit *wt* AE1 function. As was found for human AE1 Prague I [23], the mechanism appeared to be via interference with accumulation of normal protein levels at the oocyte surface. However, the stoichiometry of inhibition was not compatible with simple dominant negative effects exerted within dimeric or tetrameric units.

In summary, mutations in two previously unexamined regions of mouse AE1 led to loss-of-function phenotypes in the *Xenopus* oocyte expression system. Loss of function was secondary to decreased accumulation of the mutant polypeptides at the oocyte surface.

Acknowledgements

This work was supported by NIH Grants DK 43495 (S.L.A.) and DK 34854 to the Harvard Digestive Diseases Center and S.L.A.

References

- [1] S.L. Alper, Cell Physiol. Biochem. 4 (1994) 265–281.
- [2] R.R. Kopito, Int. Rev. Cytol. 123 (1990) 177–199.
- [3] S.L. Alper, B.E. Shmukler, J. Am. Soc. Nephrol. 6 (1995) 203a.
- [4] S. Muller-Berger, D. Karbach, J. Konig, S. Lepke, P.G. Wood, H. Appelhans, H. Passow, Biochemistry 34 (1995) 9315–9324.
- [5] Z. Wang, P.J. Schultheis, G.E. Shull, J. Biol. Chem. 271 (1996) 7835–7843.
- [6] D.N. Wang, V.E. Sarabia, R.A.F. Reithmeier, W. Kuhlbrandt, EMBO J. 13 (1994) 3230–3235.

- [7] A.R. Gargaro, G.B. Bloomberg, C.E. Dempsey, M. Murray, M.J.A. Tanner, *Eur. J. Biochem.* 221 (1994) 445–454.
- [8] L.J. Bruce, M.M.B. Kay, C. Lawrence, M.J.A. Tanner, *Biochem. J.* 293 (1993) 317–320.
- [9] P. Jarolim, J.L. Murray, H.L. Rubin, W.M. Taylor, J.T. Prchal, S.K. Ballas, L.M. Snyder, L. Chrobak, W.D. Melrose, V. Brabec, J. Palek, *Blood* 88 (1996) 4366–4374.
- [10] P. Jarolim, H.L. Rubin, V. Brabec, L. Chrobak, A.S. Zolotarev, S.L. Alper, C. Brugnara, H. Wichterle, J. Palek, *Blood* 85 (1995) 634–640.
- [11] P. Jarolim, H.L. Rubin, S.-C. Liu, V. Brabec, L. Derrick, S. Yi, S.T.O. Saad, D.E. Golan, M. Cho, S.L.Y. Alper, C. Brugnara, J. Palek, *J. Clin. Invest.* 93 (1994) 121–130.
- [12] A.E. Schofield, D.M. Reardon, M.J.A. Tanner, *Nature* 355 (1992) 836–838.
- [13] L.J. Bruce, D.J. Anstee, F.A.A. Spring, M.J.A. Tanner, *J. Biol. Chem.* 269 (1994) 16155–16158.
- [14] L.J. Bruce, S.M. Ring, D.J. Anstee, M.E. Reid, S. Wilkinson, M.J.A. Tanner, *Blood* 85 (1995) 541–547.
- [15] P. Jarolim, J.L. Murray, H.L. Rubin, E. Smart, J.M. Moulds, *Transfusion*, in press.
- [16] I. Inaba, A. Yawata, I. Koshino, K. Sato, M. Takeuchi, Y. Takakuwa, S. Manno, Y. Yawata, A. Kanzaki, J. Sakai, A. Ban, K. Ono, Y. Maede, *J. Clin. Invest.* 97 (1996) 1804–1817.
- [17] L.L. Peters, R.A. Shivdasani, S.-C. Liu, M. Hanspal, K.M. John, J. Gonzalez, C. Brugnara, B. Gwynn, N. Mohandas, S.L. Alper, S.H. Orkin, S.E. Lux, *Cell* 86 (1996) 917–927.
- [18] T. Claudio, W.N. Green, D.S. Hartman, D. Hayden, H.L. Paulson, F.J. Sigworth, S.M. Sine, A. Swedlund, *Science* 238 (1988) 1688–1694.
- [19] S.A. Cunningham, R.T. Worrell, D.J. Benos, R.A. Frizzell, *Am. J. Physiol.* 262 (1992) C783–C788.
- [20] S. Ruetz, A. Lindsey, C.L. Ward, R.R. Kopito, *J. Cell Biol.* 121 (1993) 37–48.
- [21] D. Bartel, S. Lepke, G. Layh-Schmitt, B. Legrum, H. Passow, *EMBO J.* 8 (1989) 3601–3609.
- [22] F.C. Brosius, S.L. Alper, A.-M. Garcia, H.F. Lodish, *J. Biol. Chem.* 264 (1989) 7784–7787.
- [23] M.N. Chernova, P. Jarolim, J. Palek, S.L. Alper, *J. Membr. Biol.* 148 (1995) 203–210.
- [24] M.N. Chernova, L. Jiang, D.H. Vandorpe, M. Hand, M. Crest, K. Strange, S.L. Alper, *J. Gen. Physiol.* 109 (1997) 345–460.
- [25] A.-M. Garcia, H.F. Lodish, *J. Biol. Chem.* 264 (1989) 19607–19613.
- [26] J.D. Groves, M.J.A. Tanner, *J. Biol. Chem.* 270 (1995) 9097–9105.
- [27] B.D. Humphreys, L. Jiang, M. Chernova, S.L. Alper, *Am. J. Physiol.* 268 (1995) C201–C209.
- [28] S. Lepke, A. Becker, H. Passow, *Biochim. Biophys. Acta* 1106 (1992) 13–16.
- [29] Y. Zhang, M.N. Chernova, A.K. Stuart-Tilley, L. Jiang, S.L. Alper, *J. Biol. Chem.* 271 (1996) 5741–5749.
- [30] D.M. Lieberman, R.A.F. Reithmeier, *J. Biol. Chem.* 263 (1988) 10022–10028.
- [31] T.A. Kunkel, K. Bebenek, J. McClary, *Methods Enzymol.* 204 (1991) 125–139.
- [32] S.L. Alper, J. Natale, S. Gluck, H.F. Lodish, D. Brown, *Proc. Natl. Acad. Sci. USA* 86 (1989) 5429–5433.
- [33] R.R. Kopito, H.F. Lodish, *Nature* 316 (1985) 234–238.
- [34] P.G. Wood, *Prog. Cell. Res.* 2 (1992) 325–352.
- [35] L.Y. Tam, T.W. Loo, D.M. Clarke, R.A.F. Reithmeier, *J. Biol. Chem.* 269 (1994) 32542–32550.
- [36] M.L. Jennings, *J. Gen. Physiol.* 105 (1995) 21–47.
- [37] I. Sekler, R.S. Lo, R.R. Kopito, *J. Biol. Chem.* 270 (1995) 28751–28758.
- [38] M.L. Jennings, M.P. Anderson, R. Monaghan, *J. Biol. Chem.* 261 (1986) 9002–9010.
- [39] A.S. Zolotarev, M.N. Chernova, D. Yannoukakos, S.L. Alper, *Biochemistry* 35 (1996) 10367–10376.
- [40] C.C. Wang, J.A. Badylak, S.E. Lux, R. Moriyama, J.E. Dixon, P.S. Low, *Protein Sci.* 1 (1992) 1206–1214.
- [41] C.C. Wang, R. Moriyama, C.R. Lombardo, P.S. Low, *J. Biol. Chem.* 270 (1995) 17892–17897.
- [42] I. Sekler, R.R. Kopito, J.R. Casey, *J. Biol. Chem.* 270 (1995) 21028–21034.
- [43] L. Ercolani, D. Brown, A. Stuart-Tilley, S.L. Alper, *Am. J. Physiol.* 262 (1992) F892–896.
- [44] K. Meyer-Siegler, D.J. Mauro, G. Seal, J. Wurzer, J.K. DeRiel, M.A. Sirover, *Proc. Natl. Acad. Sci. USA* 88 (1991) 8460–8464.
- [45] I. Sekler, S. Kobayashi, R.R. Kopito, *Cell* 86 (1996) 929–935.
- [46] J.D. Groves, P. Falson, M. Le Maire, M.J.A. Tanner, *Proc. Natl. Acad. Sci. USA* 93 (1996) 12245–12250.
- [47] A. Mori, K. Okubo, D. Kang, N. Hamasaki, *J. Biochem. (Tokyo)* 118 (1995) 1192–1198.
- [48] D. Kang, K. Okubo, N. Hamasaki, N. Kuroda, H. Shiraki, *J. Biol. Chem.* 267 (1992) 19211–19217.
- [49] M.L. Jennings, P.G. Gosselink, *Biochemistry* 34 (1995) 3588–3595.